April 2004

Carbon-Mediated Aggregation of Self-Interstitials in Silicon

Sumeet Kapur
University of Pennsylvania, kapurs@seas.upenn.edu

Manish Prasad
University of Pennsylvania

Talid R. Sinno
University of Pennsylvania, talid@seas.upenn.edu

Postprint version. Published in *Physical Review B* Volume 69, Number 15, 155214 (2004) (8 pages) Publisher URL: http://dx.doi.org/10.1103/PhysRevB.69.155214

Carbon-Mediated Aggregation of Self-Interstitials in Silicon

Abstract
The carbon-mediated aggregation of silicon self-interstitials is investigated with a novel approach based on large-scale parallel molecular dynamics. The presence of carbon in the silicon matrix is shown to lead to concentration-dependent self-interstitial cluster pinning, dramatically reducing cluster coalescence and thereby inhibiting the nucleation process. The extent of cluster pinning increases with cluster size for the range of cluster sizes observed in the simulation. The effect of carbon on single self-interstitials is shown to be of secondary importance, and the concentration of single self-interstitials as a function of time is essentially unchanged in the presence of carbon. A quasi-single component mean-field interpretation of the atomistic simulation results further confirms these conclusions and suggests that the experimentally observed effect of carbon on transient-enhanced diffusion (TED) could be due to carbon-cluster interactions.

Keywords
carbon, silicon, interstitials, semiconductors, diffusion

Comments
Postprint version. Published in *Physical Review B* Volume 69, Number 15, 155214 (2004) (8 pages) Publisher URL: http://dx.doi.org/10.1103/PhysRevB.69.155214

Carbon-Mediated Aggregation of Self-Interstitials in Silicon

Sumeet Kapur, Manish Prasad, and Talid Sinno[1]

Department of Chemical and Biomolecular Engineering

University of Pennsylvania

Philadelphia, PA 19104

The carbon-mediated aggregation of silicon self-interstitials is investigated with a novel approach based on large-scale parallel molecular dynamics. The presence of carbon in the silicon matrix is shown to lead to concentration-dependent self-interstitial cluster pinning, dramatically reducing cluster coalescence and thereby inhibiting the nucleation process. The extent of cluster pinning increases with cluster size for the range of cluster sizes observed in the simulation. The effect of carbon on single self-interstitials is shown to be of secondary importance, and the concentration of single self-interstitials as a function of time is essentially unchanged in the presence of carbon. A quasi-single component mean-field interpretation of the atomistic simulation results further confirms these conclusions and suggests that the experimentally observed effect of carbon on transient-enhanced diffusion (TED) could be due to carbon-cluster interactions.

PACS Numbers: 61.72.Ji, 61.72.Ss

[1] Email Address: talid@seas.upenn.edu

I. Introduction

The growth and dissolution of silicon self-interstitial clusters in the presence of carbon have attracted much attention recently because of the role of self-interstitials in the transient-enhanced diffusion (TED) of boron during post-implantation annealing and activation [1,2]. The occurrence of TED has been unambiguously attributed to the presence of supersaturated self-interstitials, which are formed during ion-implantation of dopants such as boron. The supersaturated self-interstitials are stored in clusters, which can possess a variety of morphologies, depending on the processing conditions. The most commonly observed structures are typically {311} defects [3] and dislocation-loop networks [4], but three-dimensional clusters are also possible, especially if clustering occurs at high temperatures, such as during crystal growth from the melt [].

Once formed, these clusters become unstable during thermal annealing, which is required to anneal the damage produced by boron ion-implantation and also to activate the boron atoms (i.e. allow them to occupy substitutional sites within the lattice). Cluster dissolution then leads to the observed temporary boron diffusion enhancement via the kick-out reaction $B_i \leftrightarrow B_s + I$ [5,6], where B_i and B_s represent interstitial and substitutional boron atoms, respectively, and I is a silicon self-interstitial. This TED effect leads to broadening of implanted boron profiles and poses a challenge for future CMOS device scaling goals.

The presence of high carbon atom concentrations (> 10^{19} cm^3) in the region of the self-interstitial supersaturation has been shown to greatly inhibit TED in several experimental studies,

either using highly C-doped layers grown by molecular beam epitaxy (MBE) [7] or carbon co-implantation with the boron [8]. While the use of carbon to inhibit TED continues to be plagued by technological difficulties [7], promising new approaches currently are being evaluated that make a fundamental understanding of carbon-mediated TED of immediate importance [9]. A recent example is to implant carbon atoms and create an embedded layer that does not interact with the surface device-active region, alleviating the previously reported detrimental effects of carbon on the electrical properties of microelectronic devices.

Numerous computational TED-related studies have been reported in the literature. These studies have employed approaches ranging from macroscopic rate equation simulations [7], to kinetic Monte Carlo calculations (KMC) [10], to detailed atomistic studies of the energetics and structure of various carbon-silicon complexes [11]. The former two approaches typically have focused on the role of single self-interstitial (I), trapping by carbon (C), via the reactions

$$C_S + I \leftrightarrow C_I , \tag{1}$$

$$C_S + C_I \leftrightarrow C_S C_I . \tag{2}$$

where, C_S, and C_I, denote substitutional and interstitial carbon atoms, respectively. The validity of rate equation and KMC models for carbon-mediated self-interstitial diffusion has been tested against experiments that measure the effective self-interstitial diffusivity using doped marker layers [12] or metal tracer diffusion [13]. In general, good agreement between the models and experimental data is obtained but it has not been possible to assess the robustness or completeness of the assumed mechanisms.

Recently it has been speculated that additional pathways involving the formation of clusters of self-interstitials and carbon atoms may be important [14]. However, the co-precipitation of carbon and silicon interstitials requires, in principle, the consideration of a two-dimensional cluster array of the form $C_n I_m$. An atomistic characterization of every cluster species and reaction pathway, e.g. $C_2I + I \leftrightarrow C_2I_2$, rapidly becomes computationally intractable because of the large number of species and possible configurations that must be considered.

In this paper, an alternative approach based on parallel molecular dynamics (PMD) is presented that allows for a detailed analysis of the effect of carbon on self-interstitial aggregation without the need to consider every cluster composition or configuration individually. In essence, the averaging over composition and configuration space is automatically performed within the MD simulation if a sufficient number of atoms are considered. At the same time, full atomic resolution is provided throughout the entire simulation, and no assumptions, other than the validity of the interatomic potential, are needed. The remainder of the paper is organized as follows. The details of the MD simulations and basic results are described first in Section II. Also discussed in this section are the major assumptions of the approach, with emphasis on the choice of interatomic potential. The results of the aggregation simulations are presented and discussed in Section III. In Section IV, the parallel MD results and additional atomistic simulations of cluster mobility are interpreted in the context of a mean-field model which suggests that it might be possible to treat the carbon-in-silicon system as a quasi-single component system where the carbon atoms are considered implicitly through their effects on the properties of the self-interstitial clusters. Finally, conclusions are presented in Section IV.

II. MD Simulation of Carbon and Self-Interstitial Aggregation

Two large-scale parallel MD (PMD) simulations were carried out using systems of 216,000 silicon atoms, each containing an additional 1,000 self-interstitials initially placed in uniformly spaced (and isolated) tetrahedral sites. In the second simulation cell, 2,000 randomly selected silicon lattice atoms were replaced with substitutional carbon atoms, corresponding to a 0.9% carbon concentration or 4×10^{20} cm^{-3}. These large concentrations of self-interstitials and carbon atoms were chosen to allow the systems to exhibit sufficient aggregation in the short MD time scale (nanoseconds). While the high concentrations do affect the overall rate of aggregation, it should be noted that there is no reason to expect that the fundamental micro-processes predicted by the interatomic potential should be altered in a qualitative way. This issue is addressed further in a later section.

A. Simulation Conditions

In both NVT simulations, the temperature and pressure were fixed at 2650 K and zero, respectively. The Tersoff set of empirical potentials for silicon are well-known to greatly overestimate the melting temperature, and 2650 K was found to be about 600-800 K below the mechanical melting point. A direct comparison of this temperature to experimental annealing temperatures (typically around 900 ºC) is not possible, but a consistent estimate can be made based on the self-interstitial diffusion coefficient. A very good estimate for the self-interstitial diffusivity recently has been provided by model regression to several experimental observations including the diffusion of zinc into Si wafers at various temperatures and the formation of the so-

called interstitial-vacancy boundary during Czochralski crystal growth [15]. Comparison of this value to the Tersoff prediction indicates that 2650 K is approximately equivalent to an actual temperature of 1000 ºC, which is in the neighborhood of typical annealing temperatures in TED experiments. Note that this is not a unique assignment of the simulation temperature, but is a relevant one for a study of self-interstitial diffusion and aggregation phenomena.

B. Validity of the Tersoff Multicomponent Empirical Potential

The multicomponent Tersoff potential [16] was used for all simulations, along with the potential parameters specified by Tang and Yip [17]. This potential is one of very few available for multicomponent Group IV systems, and, given the relatively small number of studies of multicomponent systems (relative to pure silicon, for example), it is somewhat more difficult to estimate the uncertainties in the following simulations. However, several previous studies employing this empirical potential have shown that it is surprisingly accurate at predicting structure and properties of silicon-carbon complexes.

In an excellent study of carbon-silicon defect complex formation, Mattoni et al. [] used a combination of empirical potential MD and DFT (in the local density approximation) calculations to investigate energetics and reaction pathways. Steps of the reaction sequence $C_S + I \rightarrow C_I + C_S \rightarrow C_S C_I + I \rightarrow C_I C_I$ were analyzed in detail by computing system energies as each pair of species were brought together. In each case, the energy profile for the reaction path obtained with LDA-DFT and the empirical Tersoff potential were qualitatively similar, and in some cases almost identical. Local energy minima in the first and third reactions shown above

predicted by the DFT calculations also were captured by the Tersoff potential. These results indicate that this empirical potential should be suitable for use in the current study. Additional evidence supporting the qualitative accuracy of the multicomponent Tersoff potential was suggested by the calculations of Tersoff, in which the formation energies and diffusivity of carbon complexes in silicon were found to be in good agreement with experimental solubility data []. These results were later supported by LDA-DFT calculations [].

III. Characterization of Interstitial Aggregation

A. Identification of Interstitial Clusters

Aggregation during the two PMD simulations was monitored periodically using snapshots of the entire configuration of each system. For each snapshot, the configurations were first quenched using conjugate gradient energy minimization in order to make identification of the defect clusters easier. The quenched coordinates were then used to identify individual clusters and generate a size distribution at each time point. A substantial difficulty in the identification of interstitial clusters arises because of the extent of lattice distortion in the vicinity of interstitial atoms. In fact, up to several atoms can be substantially displaced from their equilibrium positions in the presence of a single silicon self-interstitial [] and, for the compact structures that were generated in our simulations, the displacements do not follow a regular pattern. Furthermore, it was readily apparent that these displacements were equal in magnitude to the distance of a self-interstitial from the nearest lattice site – i.e. in a cluster of self-interstitials,

it is not possible to uniquely identify which atoms are interstitials and which ones are simply displaced atoms.

This issue was addressed by the identification of *Defective Atoms* (DAs), defined as Si or C atoms that are at least θ% of a bond length (2.35 Å) from the nearest lattice position. For a given value of the parameter θ, DAs were identified by comparison of the quenched simulation coordinates to a perfect lattice at the same density. Subsequently, the DAs were assigned to individual clusters using a recursive algorithm []. The assignment of atoms to individual clusters requires that an interaction distance, β, be defined. Thus, sets of atoms that are connected by β belong to the same cluster. For given values of θ and β, a cluster size distribution based on defective atoms can be defined – note that this is not equivalent to the *interstitial* cluster size distribution. The latter was computed in the following manner. Each defective atom cluster was isolated and the atomic coordinates within the cluster compared to a reference lattice. The number of excess atoms in the cluster gives the number of interstitials contained within the cluster. This number is then used to recompute the interstitial cluster size distribution. Finally note that no distinction is made between carbon and silicon interstitials in the carbon-doped case (XXX – HOW DOES THIS AFFECT THE SIZE DIST???).

Previous atomistic investigations [] have suggested that the interaction distance between two silicon self-interstitials extends to the 3rd-nearest neighbor (3NN) distance. In the present case, however, this interaction distance is not directly applicable because of the ambiguity in defining interstitial atoms. Note that once the DA interaction distance, β, is specified and a cluster identified, the interstitial interaction distance is no longer relevant because all the

interstitials in that cluster are automatically assumed to be connected. We have performed a detailed sensitivity analysis of the effect of β and θ on the resulting size distribution that will be presented in Section IV. Here, we simply note that the resulting distribution is only weakly dependent on the choice of these parameters, at least within physically reasonable bounds.

B. Structure of Interstitial Clusters

The quenched configurations at 3.46 ns for the pure silicon and 0.9 % carbon-in-silicon simulations are shown in Figures 1(a) and 1(b), respectively. Shown are *Defective Atoms* (DAs), as defined by $\theta = XXX\%$ and $\beta = 4.82$ Å , corresponding to the 3NN distance. The pure silicon case shows substantially greater cluster size evolution with fewer, but much larger, clusters as compared to the 0.9% C-doped case. This result is consistent with the notion that carbon reduces the effective diffusivity of self-interstitials and therefore inhibits the cluster ripening (or dissolution) process. This effect also has been observed in the float-zone growth of silicon crystals, where carbon doping was observed to increase the density, but decrease the size, of interstitial-type aggregates [18].

The structure of the DA clusters in Figure 1 appears to be different in the two simulations, with the clusters in the pure Si case appearing to be more spherical. This observation was tested in more detail by computing moments of inertia for each cluster in both cases, which can be used to quantitatively estimate the aspect ratio of each cluster. In Figure 2, the averaged moment of inertia ratios are shown for both simulations and it is clearly seen that the pure Si clusters are indeed more spherical than in the carbon-doped case. A possible

explanation, which will be verified later in this paper, is that the carbon atoms locally pin the cluster and prevent it from rearranging to minimize its surface area, at least in the timescales accessible to MD simulation. (HOW ABOUT C-C INTERACTION WITHIN THE CLUSTERS???XXX)

The number of DAs in each simulation is not a conserved quantity and can evolve in time. The number of DAs per cluster, n_{DA}, is shown in Figure 3 as a function of interstitial cluster size, n_I, for both carbon concentrations. In both cases, n_{DA} is well represented by a power-law evolution across the entire interstitial cluster size range $(1 < n_I < 130)$ but interestingly, has an exponent larger than one: approximately 1.17 for the pure Si case, and 1.07 for the carbon-doped case. The slightly lower exponent for larger clusters in the carbon-doped case is likely due to the compressive strain relief that carbon atoms provide because of their smaller size. The non-linear increase of n_{DA} with cluster size implies that as the size distribution coarsens, the total number of DAs increases and therefore should provide a driving force against coarsening, which could lead to self-limiting of the coarsening process at later times. It is possible that this process might provide a driving force for the hypothesized morphological transformation of compact clusters to dislocation loop networks – the latter are the only observed structures in interstitial-rich silicon grown from the melt []

IV. Size Distribution Evolution and Mean-Field Modeling

The time evolution of the average interstitial cluster size for the pure silicon and carbon-doped MD simulations are shown in Figure 4. The average cluster size is defined here as

M_2 / M_1, where $M_n = \sum_s s^n X_s$ and X_s is the number of clusters of size s. Both evolutions show an initial lag followed by the establishment of power-law scaling, $\sim t^z$, with the pure silicon case clearly exhibiting much faster evolution than the C-doped system (exponents are 0.81 and 0.37, respectively).

The distributions of small clusters ($n \leq 4$) for both cases are plotted in Figure 5. Interestingly, the single self-interstitial profiles are essentially identical throughout the simulation, indicating that *the presence of carbon does not substantially affect the transport of single self-interstitials*. However, for dimers and tetramers, substantial divergence between the pure Si and C-doped simulations can be observed after 200 ps of simulation time. The extent of the divergence appears to increase with cluster size – in fact, for the duration of the simulation, the tetramer concentration in the carbon-doped case is essentially constant and only begins to drop at the end of the simulation after reaching a maximum at 100 ps. In contrast the tetramer profile in the pure Si case rapidly decreases, indicating growth to larger sizes.

A. Mean-Field Scaling Approximation for Aggregation

The power-law scaling of the average cluster sizes in Figure 4 suggest that a mean-field scaling analysis might be appropriate for compactly describing the carbon effect at the continuum scale. As discussed earlier, the co-existence of carbon and silicon atoms generally implies that a two-dimensional cluster representation is necessary to describe the evolution profiles. However, here we show that an effective medium formulation is appropriate, in which the carbon atoms simply modify the properties of self-interstitial clusters. The successful

application of mean-field scaling theory to (single-component) defect aggregation has already been demonstrated by us in previous work []. A transformation proposed by Family et al. [19], and later by Sorensen et al. [20], leads to the collapse of the Smoluchowski equation for a one-dimensional (single component) cluster system,

$$\frac{dX_k}{dt} = \frac{1}{2}\sum_{i+j=k}\left[K(i,j)X_iX_j - F(i,j)X_{i+j}\right] - \sum_{j=1}^{\infty}\left[K(k,j)X_kX_j - F(k,j)X_{k+j}\right], \qquad (3)$$

into a single ordinary differential equation for the scaled average size, s^*:

$$\frac{ds^*}{dt^*} = s^{*\lambda} - s^{*(\alpha+2)}. \qquad (4)$$

In eq. (3), *K(i,j)* is the coagulation rate between two clusters of size *i* and *j*, and *F(i,j)* is the rate of dissociation of a cluster of size *i+j* into two clusters of size *i* and *j*. Implicit in the derivation of eq. (4) is that the coagulation and fragmentation kernels, *K(i,j)* and *F(i,j)*, are homogeneous, i.e. $K(ai,aj) = a^{\lambda}K(i,j)$ and $F(ai,aj) = a^{\alpha}F(i,j)$.

In eq. (4), $s^*=s(t)/s_0$ and $t^*=t/t_0$, where s_0 and t_0 are the equilibrium average cluster size, and the characteristic time to reach this equilibrium, respectively. For very small times, i.e. when $s^* << 1$, and assuming that fragmentation is not important at this stage of the evolution, the solution of eq. (4) is given by

$$s^* = \left[(1-\lambda)t^* + s_i^{*(1-\lambda)}\right]^z, \tag{5}$$

where $s_i^* = s\ (t=0)/s_0$ is the scaled initial value of the mean cluster size, and $z = 1/(1-\lambda)$. Equation (5) implies that the average size should evolve as $s^* \sim t^z$, once the first term becomes sufficiently large [21]. Now, assuming that the entire aggregation process is diffusion-limited, the coagulation kernel, *K(i,j)*, is proportional to

$$K(i,j) \sim (D_i + D_j)(r_i + r_j)^2, \tag{6}$$

where r_x and D_x (x=i,j) are the capture radius and diffusivity, respectively, of a cluster of size x. Requiring that this kernel be homogenous is equivalent to requiring that both the capture radius and diffusivities also be homogenous in the cluster size.

B. Capture Radius Model for Interstitial Clusters and Scaling Predictions

The capture radius of a cluster is usually closely related to its size assuming that there are no long-range effects transmitted through the lattice. Here, we assume that the capture zone of an interstitial cluster is given approximately by number of DAs contained within the cluster. The data in Figure 3 gives $r_{cap}(n) \sim n^{0.39}$ and $r_{cap}(n) \sim n^{0.36}$ for the pure silicon and carbon-doped cases, respectively, where n is the number of interstitials in a spherical cluster. Note that the actual capture radius of the cluster is not required and only the scaling behavior is needed for the

mean-field analysis. Further assuming that $D_{\gamma i} = \gamma^{p} D_i$, and using eq. (6), the homogeneity condition for each case can be written as,

$$K(\gamma i, \gamma j) = \gamma^{p+0.78} K(i, j), \quad (C = 0), \tag{7}$$

$$K(\gamma i, \gamma j) = \gamma^{p+0.72} K(i, j), \quad (C = 0.9\%). \tag{8}$$

The exponents for M_2 / M_1 from Figure 2 can now be used to determine *p*, which represents the decay rate of the effective cluster diffusion coefficient as a function of size *as predicted by the mean-field scaling approximation*: $D_n(C = 0) \sim n^{-1.01}$ and $D_n^{eff}(C = 0.9\%) \sim n^{-2.42}$. Thus, the mean-field model indicates that power-law evolution of the average cluster size with exponents 0.81 and 0.37, requires that cluster diffusivity must decay with cluster size as stated above. In other words, the observed carbon effect can be explained purely on the basis of cluster diffusion inhibition. Note that the mean-field scaling analysis does not require that single interstitial diffusion be altered, a result that is consistent with the profiles shown in Figure 4.

C. Atomistic Studies of Interstitial Cluster Diffusion

In order to test the hypothesis that carbon acts via cluster pinning as well as the overall validity of the scaling analysis in the previous section, a sequence of cluster diffusion measurements was performed using lengthy (7-20 million time steps) MD simulations. One to six self-interstitials were placed in a host lattice containing up to 1,000 lattice atoms, depending

on the size of the cluster and the desired carbon concentration. For each case, zero to four silicon lattice atoms were replaced by carbon atoms. Between 5 and 8 simulations were performed for every situation in order to increase the statistical accuracy of the results. The mean-square displacement (MSD) of each cluster center-of-mass was computed by periodically quenching the simulation cell and locating DAs.

Interstitial cluster diffusivity in the presence of carbon needs to be carefully defined. Our approach in the mean-field modeling was to consider the carbon implicitly via its effect on the cluster properties. In other words, the carbon atoms were considered as part of an effective medium that changes as the carbon concentration is varied. Therefore, in the diffusion runs, we do not make a distinction between the various cluster configurations and compositions, but rather, are interested only in the overall diffusivity of the cluster averaged over all possible configurations. In order to ensure that all important carbon-interstitial cluster configurations were adequately sampled, several diffusion runs were performed for each interstitial cluster, in which the total system size was varied but the carbon concentration was fixed. The diffusion measurement simulation conditions are summarized in Table 1. In all cases, intervals in which the cluster was observed to fragment into two or more sub-clusters were discarded from the overall MSD calculation.

Diffusion coefficients for clusters containing up to six self-interstitials in varying background carbon concentrations are shown in Figure 6, along with power-law fits. It is immediately apparent that the power-law fit is appropriate for all carbon concentrations for the cluster sizes considered here. Furthermore, the decay exponent becomes dramatically more

negative with increasing carbon concentration, as predicted by the mean-field scaling analysis in the previous section. Interestingly, we find once again that the effect of carbon on the diffusivity of a single self-interstitial is quite small compared to the large reduction observed in the case of the larger clusters, once again this finding is consistent with the monomer evolution profile in Figure 5 and further confirms the fact that carbon-inhibition of interstitial aggregation (and dissolution) arises from the pinning of interstitial *clusters*, rather than single self-interstitials!

The exponents of the power-law fits for the diffusion coefficients as a function of cluster size are shown in Figure 7 as a function of background carbon concentrations. First, note that simulations performed in different simulation cell sizes but at equal carbon concentration lead to the same effective diffusion coefficients, strongly indicating that our quasi-single component analysis is appropriate. The fitted curve gives a diffusivity decay exponent of –2.XX at 0.9% carbon doping and –1.06 for the pure Si case. Both of these values are in excellent quantitative agreement with the mean-field scaling predictions and indicate that the analysis is appropriate, at least for the range of cluster sizes encountered in the PMD simulations. Note that even though only small clusters containing up to six interstitials were considered in the diffusion runs, the fact that the PMD simulations predict a single power-law exponent until 4 ns of simulation time is evidence that the diffusion of larger clusters will continue to exhibit the behavior shown in Figure 6. After 4 ns of evolution, clusters containing up to XXX interstitials were observed.

V. Sensitivity Analysis of Cluster Identification

A. Sensitivity to Empirical Potential Model

The analysis presented in the previous sections depends on the validity of several assumptions. The aim of this section is to address some of these and determine the sensitivity of our conclusions to various uncertainties. The most fundamental of these is the choice of the Tersoff multicomponent potential. As mentioned previously, few empirical potentials exist for the carbon-silicon system []. We believe that the evidence cited in Section XXX is sufficient to give us reasonable confidence in the applicability of the multicomponent potential , assuming that the overall interstitial aggregation picture is at least qualitatively captured by the potential. In order to test this assumption, we used another empirical potential for pure silicon (EDIP) to simulate the aggregation of an identical system as the pure silicon case described earlier. The temperature of the EDIP simulation was chosen to be XXX K, which is the temperature at which the single self-interstitial diffusivity matched the Tersoff value at 2650 K. The predicted evolutions of the average cluster size (M2/M1), the total cluster number (M0), and the number of tetramers (X4) are shown in Figure 8, along with the Tersoff predictions. In all cases, the evolutions are qualitatively similar and only deviate at later times. The EDIP potential appears to predict slightly more rapid evolution, with the largest difference appearing in M0. This difference is due to a more rapid consumption of single interstitials in the EDIP case. The differences can be attributed to differences in the relative energies of each cluster size as well as the cluster diffusivities, most likely indicating that EDIP cluster diffuse slightly faster than Tersoff ones.

B. Sensitivity to Defective Atom Identification

The threshold displacement for identifying a defective atom in the previous results was set to $\theta = XXX$. Here we demonstrate that while the number of DAs per cluster, n_{DA}, is quite sensitive to changes in θ, the resulting interstitial cluster size distribution is only weakly affected. The number of DAs per cluster for different displacement thresholds is shown in Figure 9, and demonstrates the sensitivity of the presumed cluster size to this parameter. Note however, that the power-law scaling of n_{DA} is unchanged, which implies that the mean-field analysis in Section XXX would, in any case, be unaffected by this sensitivity. In order to predict the full size distribution at the continuum level, an absolute capture radius would be required and this issue is discussed in detail in a future publication. Another important point to note is that for all thetas considered in Figure 9, all 1,000 of the excess atoms were located at each time snapshot. Obviously, for very large values of θ, some of the interstitial atoms would be missed, and this sets a (weak) upper bound on θ. Values of θ lower than XXX led to most of the atoms in the simulation cell being tagged as defective. Physically, this percolation observation is not consistent with the mean-field interpretation and therefore $\theta = XXX$ can be taken as a strict lower bound.

The question of how the choice of θ affects the predicted *interstitial* cluster size distribution was addressed next. The sensitivity of the average cluster size and total cluster number with respect to θ is shown in Figure 10. The predicted cluster size distribution is seen to depend only weakly on the choice of θ, and even then, only for small times. In fact, the

exponent of the power-law evolution of M2/M1 varies from the base value by only 2-3% when $\theta = XXX$ and the mean-field scaling analysis is therefore unaffected by the uncertainty in the value of θ.

VI. Conclusions

The results in this paper provide a new view into the technologically and scientifically interesting TED inhibition effect of carbon doping. No assumptions are made other than the validity of the multicomponent Tersoff potential which has been tested extensively for this system [12]. Carbon is conclusively demonstrated to inhibit cluster diffusion rather than single self-interstitial transport and the overall effect on aggregation can be described well by a simple one-component mean-field representation. The results should be useful for constructing robust, but simple, rate equation models for carbon mediated self-interstitial aggregation/dissolution.

We gratefully acknowledge financial support from the National Science Foundation (CAREER CTS01-34418) and the ACS Petroleum Research Fund (No. 36923-G5).

References

[1] N.E.B. Cowern, K.T.F. Jansen, and H.F.F. Los, J. Appl. Phys. **68**, 6191 (1990).

[2] H. Ruecker, B. Heinemann, D. Bolze, R. Kurps, D. Krueger, G. Lippert, and H. J. Osten, Appl. Phys. Lett. **74**, 3377 (1999).

[3] D. Stiebel, P. Pichler and N. E. B. Cowern, Appl. Phys. Lett. **79**, 2654 (2001).

[4] D.J. Eaglesham, P.A. Stolk, H.-J. Gossmann, and J.M. Poate, Appl. Phys. Lett. **65**, 2305 (1994).

[5] C.S. Nichols, C.G. Van de Walle, and S.T. Pantelides, Phys. Rev. Lett. **62**, 1049 (1989).

[6] N.E.B. Cowern, K.T.F. Janssen, G.F.A. van de Walle, and D.J. Gravesteijn, Phys. Rev. Lett. **65**, 2434 (1990).

[7] S. Mirabella, A. Coati, D.De Salvador, E. Napolotani, A. Mattoni, G. Bisognin, M. Berti, A. Carnera, A.V. Drigo, S. Scalese, S. Pulvirenti, A. Terrasi, and F. Priolo, Phys. Rev. B **65**, 045209 (2002).

[8] A. Cacciato, J.G.E. Klappe, N.E.B. Cowern, W. Vandervost, L.P. Biro, J.S. Custer, and F.W. Saris, J. Appl. Phys. **79**, 2314 (1996).

[9] E. Napolotani, A. Coati, D.De Salvador, A. Carnera, S. Mirabella, S. Scalese, and F. Priolo, Appl. Phys. Lett. **79**, 4145 (2001).

[10] M.D.Johnson, M.-J.Caturla, and T.Diaz de la Rubia, J. Appl. Phys. **84**, 1963 (1998).

[11] A. Mattoni, F. Bernardini, and L. Colombo, Phys. Rev. B **66**, 195214 (2002).

[12] H.-J. Gossmann, C. S. Rafferty, H. S. Luftman, F. C. Unterwald, T. Boone, and J. M. Poate, Appl. Phys. Lett. **63**, 639 (1993).

[13] P. Laveant, P. Werner, G. Gerth, U. Goesele. Diffusion & Def. Data Pt. B: Sol. State Phenom. **82-84**, 189 (2002).

[14] R. Pinacho, P. Castrillo, M. Jaraiz, I. Martin-Bragado, J. Barbolla, H.-J. Gossmann, G.-H. Gilmer, and J.-L. Benton, J. Appl. Phys. **92**, 1582 (2002).

[15] T. A. Frewen, T. Sinno, R. Hoelzl, W. von Ammon, and H. Bracht, J. Electrom. Soc. In press (expected in print 08/2003).

[16] J.Tersoff, Phys. Rev. B **39**, 5566 (1989); also see J.Tersoff Phys. Rev. B **41**, 3248 (1990); J.Tersoff, Phys. Rev. Lett. **64**, 1757 (1990).

[17] M. Tang and S. Yip, Phys. Rev. B **52**, 15150 (1995).

[18] H. Foll, U. Gosele, and B.O. Kolbesen, in Semiconductor Silicon, eds: H.R. Huff and E. Sirtl, Vol. **77-2**, 565 (The Electrochemical Soc., Princeton, NJ, 1977).

[19] F.Family, P.Meakin, and J.M.Deutch, Phys. Rev. Lett. **57**, 727 (1986).

[20] C.M. Sorensen, H.X. Zhang, and T.W. Taylor, Phys. Rev. Lett. **59**, 363 (1987).

[21] M. Prasad and T. Sinno, Phys. Rev. B In press (expected in print 08/2003)

FIG. 1. Distribution of Defective Atoms (DAs) at $t = 3.46$ ns. (a) pure Si (4337 DAs), and (b) 0.9% C-doped Si (3164 DAs). Note that the number of DAs is much greater than the number of interstitials (1000) because of lattice strain effects.

FIG. 2. Moments of Inertia.

FIG. 3. Number of defective atoms (n_{DA}) as a function of number of interstitials in a cluster (n_I): pure Si (circles with thick solid line), 0.9% carbon-doped (squares with dash line). The thin solid line shows linear evolution for reference.

FIG. 4. Evolution of the average interstitial cluster size, M_2 / M_1, for pure Si (solid squares) and 0.9% C-doped Si (open squares). Exponents of the power-law fits are 0.81 for pure Si (solid line) and 0.38 for 0.9% C-doped Si (dashed line).

FIG. 5. Evolution profiles for interstitial clusters of size 1,2 and 4. Pure Si - filled symbols, 0.9% C-doped Si - open symbols. Tetramer profile is based on the right-hand side axis for clarity.

FIG. 6. Self-interstitial diffusivities as a function of size with varying carbon concentrations. (a) 0% C, (b) 0.2 % C, (c) 0.4 % C, and (d) 0.8 % C.

FIG. 7. Exponents for the power-law fits of cluster diffusion decay as a function of cluster size.

FIG. 8. Evolution of the average cluster size (squares), total cluster number (diamonds), and dimers (triangles) using the Tersoff (solid symbols), and EDIP (open symbols) potentials.

FIG. 9. Number of defective atoms (n_{DA}) as a function of cluster size for different values of the threshold parameter, θ: $\theta = XXX$ (squares), (b) $\theta = XXX$ (circles), (c) $\theta = XXX$ (triangles).

FIG. 10. Sensitivity of the computed size distribution to the threshold parameter, θ. $\theta = XXX$ (squares), (b) $\theta = XXX$ (circles), (c) $\theta = XXX$ (triangles).

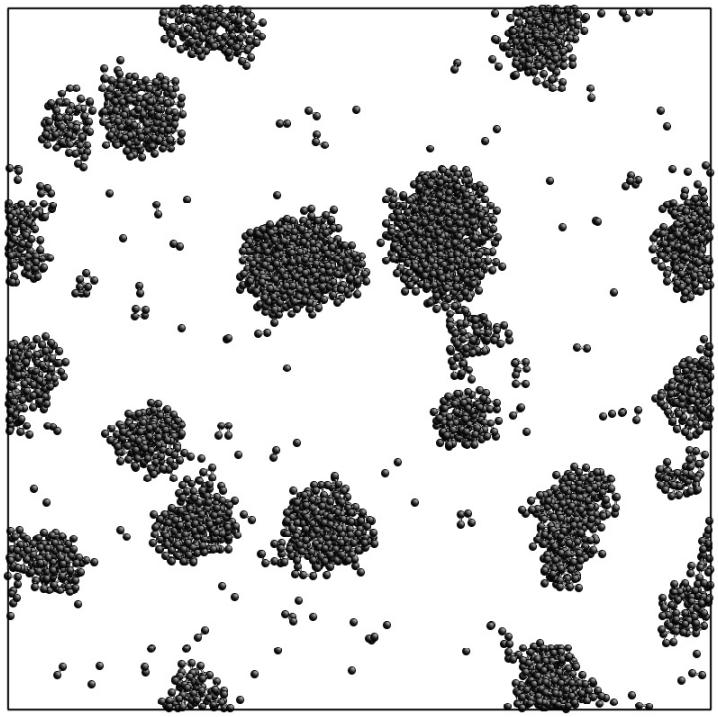

Figure 1(a): Kapur, Prasad, and Sinno

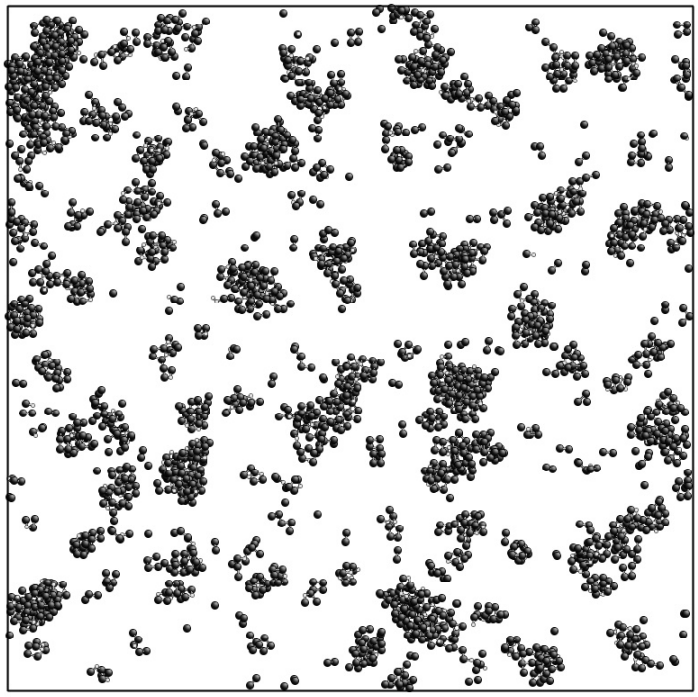

Figure 1(b): Kapur, Prasad, and Sinno

Figure 2: Kapur, Prasad, and Sinno

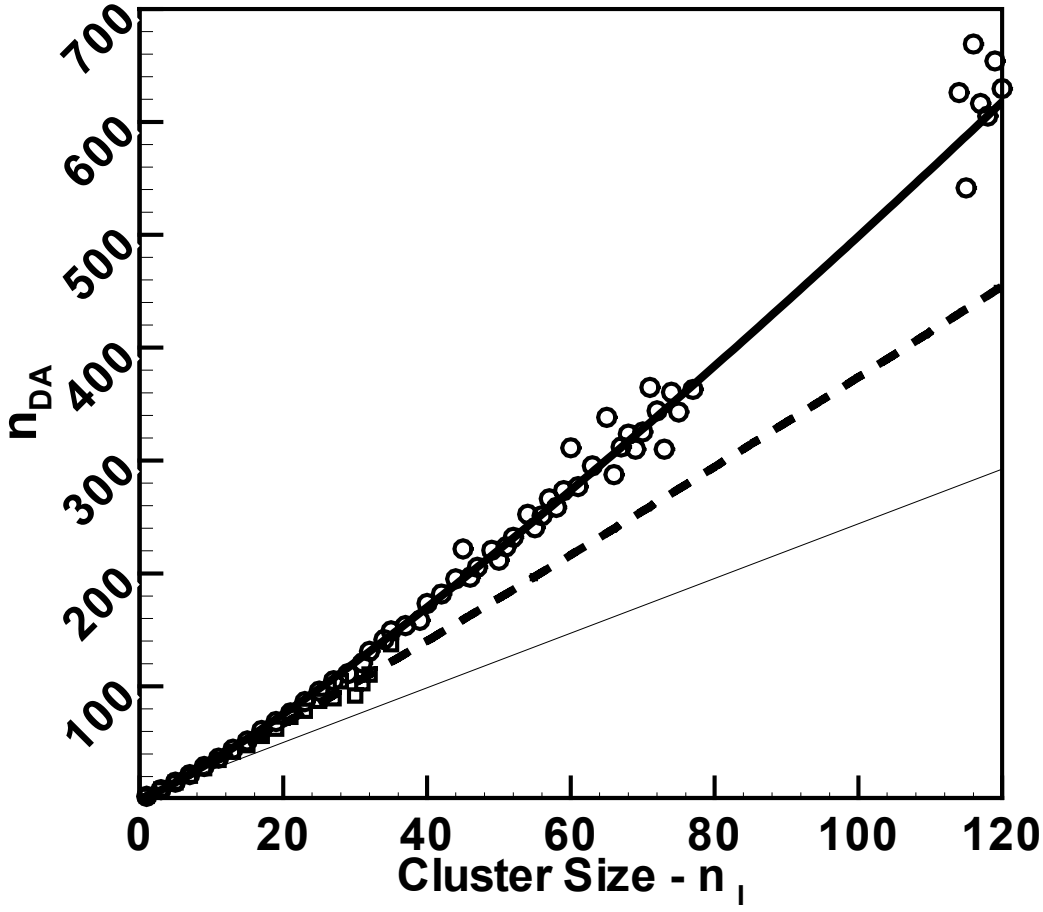

Figure 3: Kapur, Prasad, and Sinno

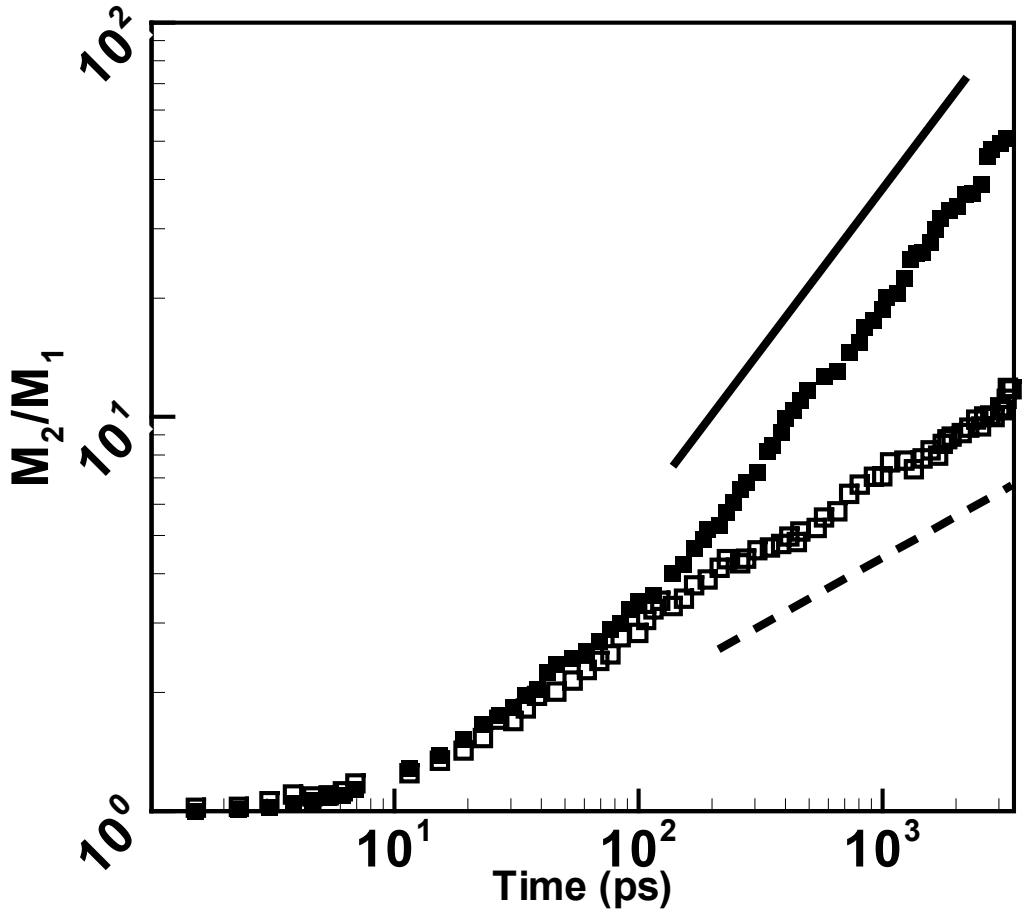

Figure 4: Kapur, Prasad, and Sinno

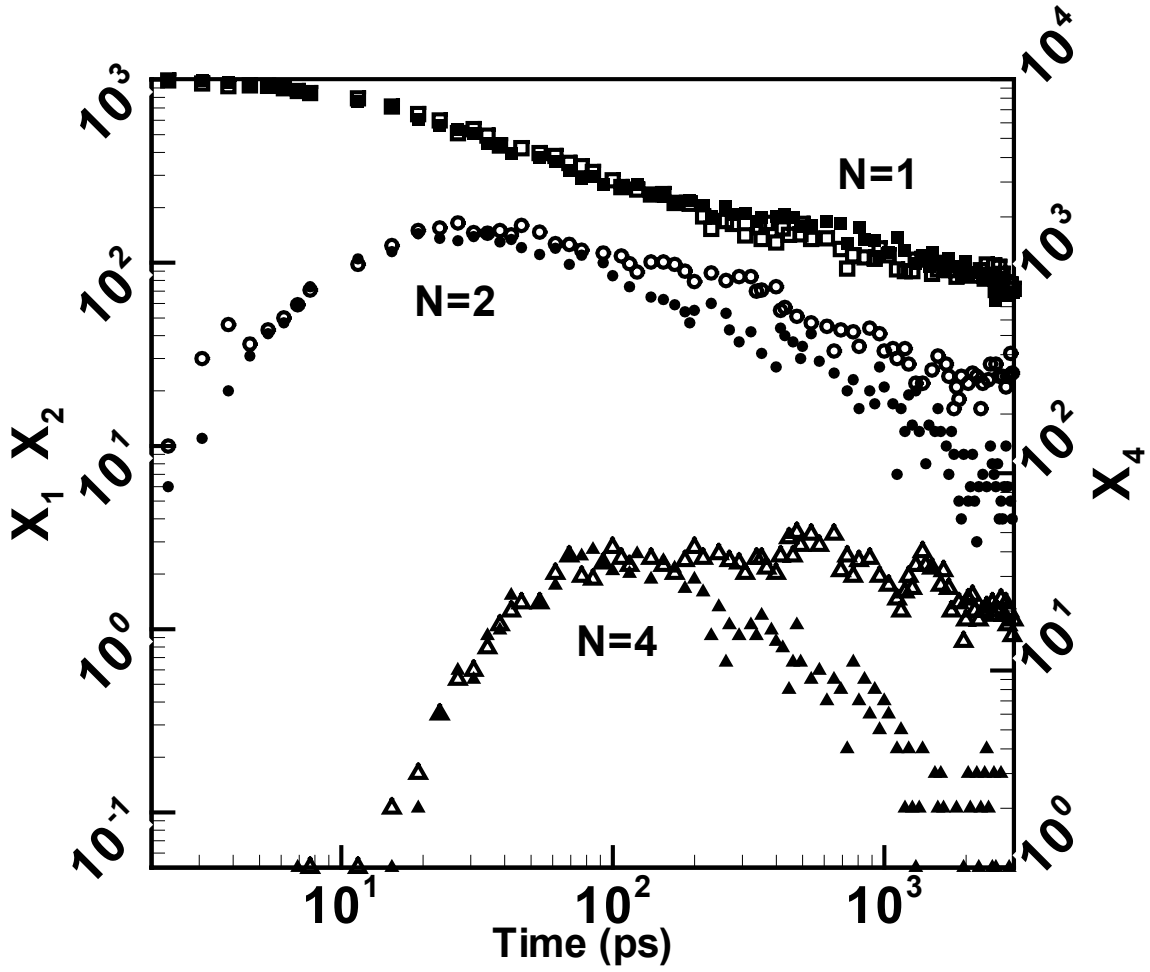

Figure 5: Kapur, Prasad, and Sinno

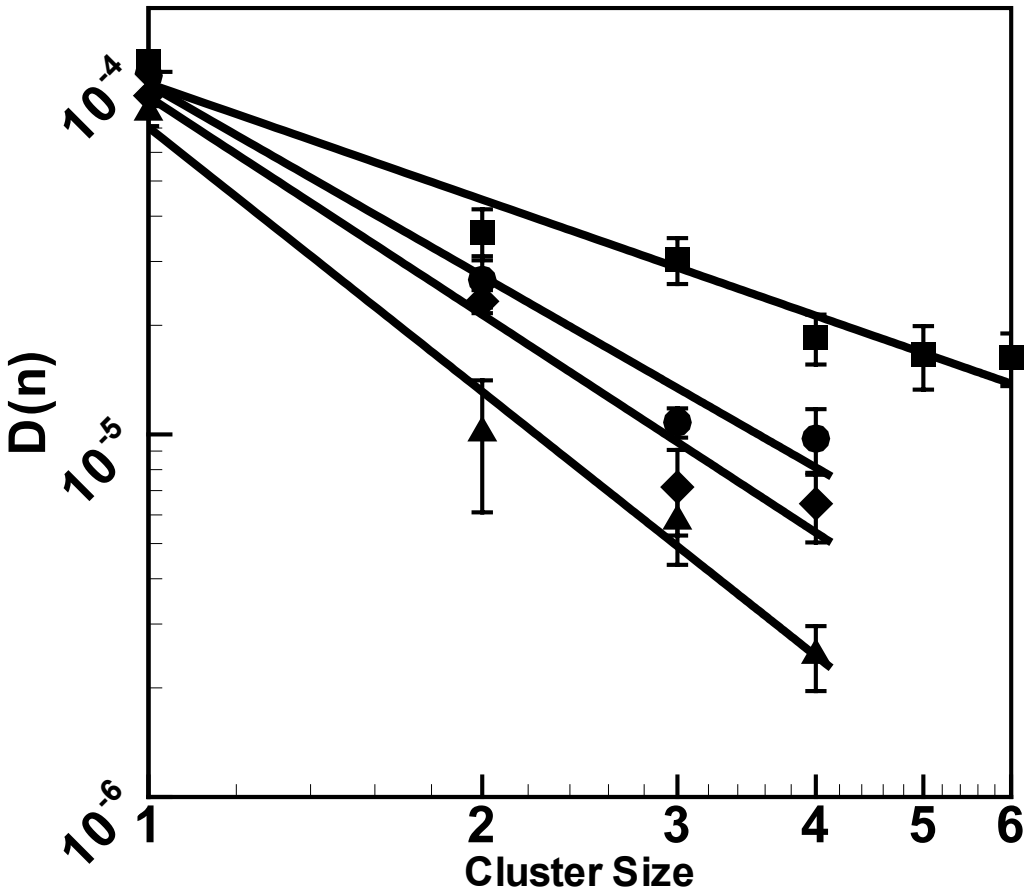

Figure 6: Kapur, Prasad, and Sinno

Figure 7: Kapur, Prasad, and Sinno

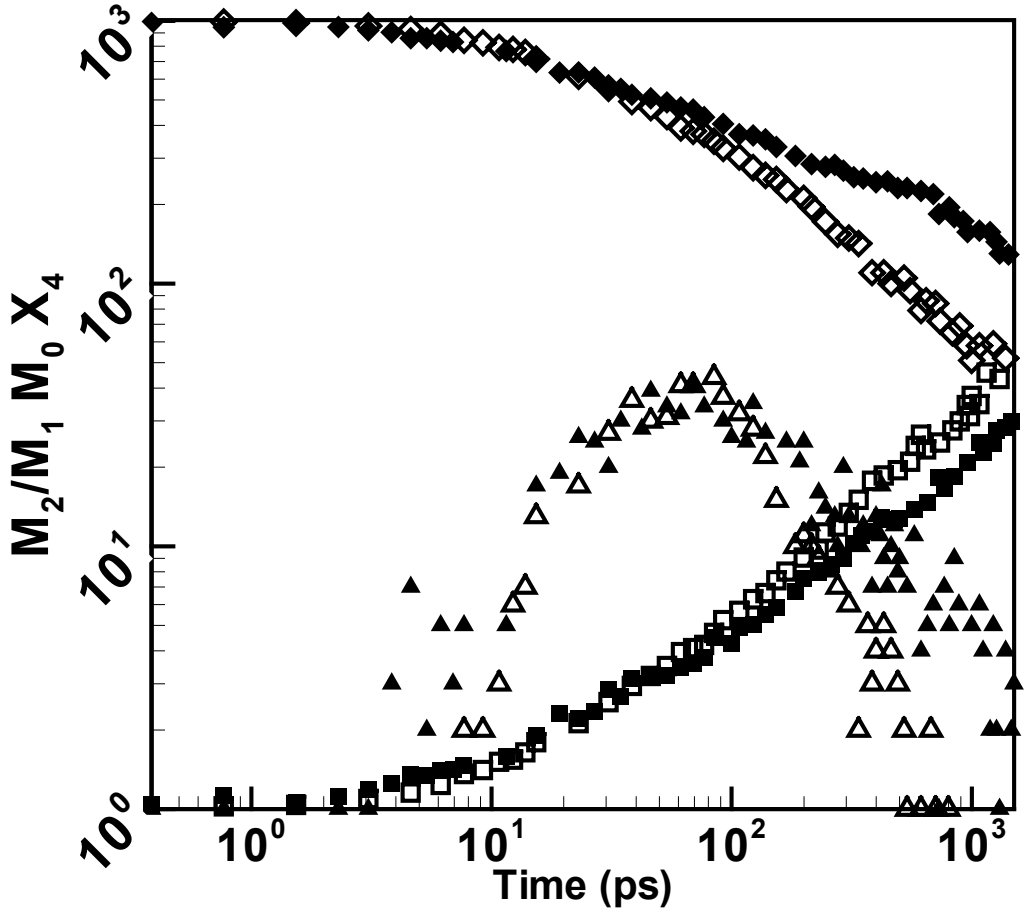

Figure XXX: Kapur, Prasad, and Sinno

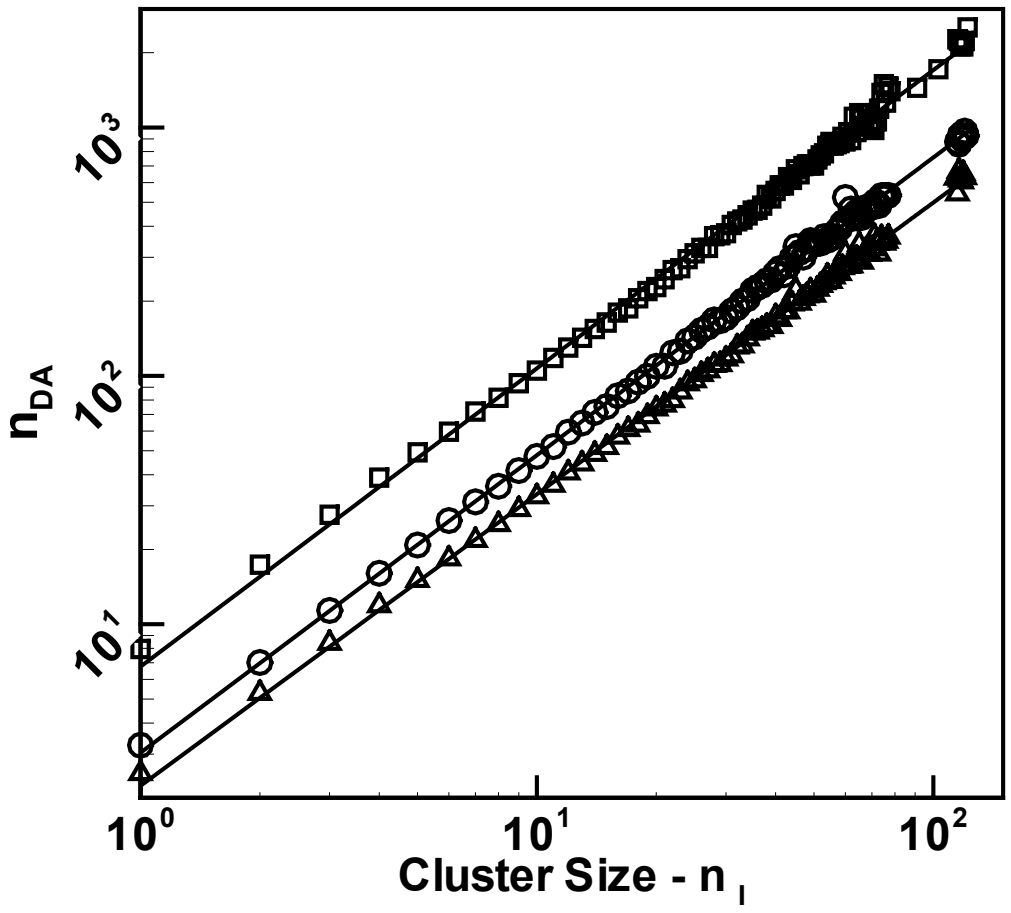

Figure XXX: Kapur, Prasad, and Sinno

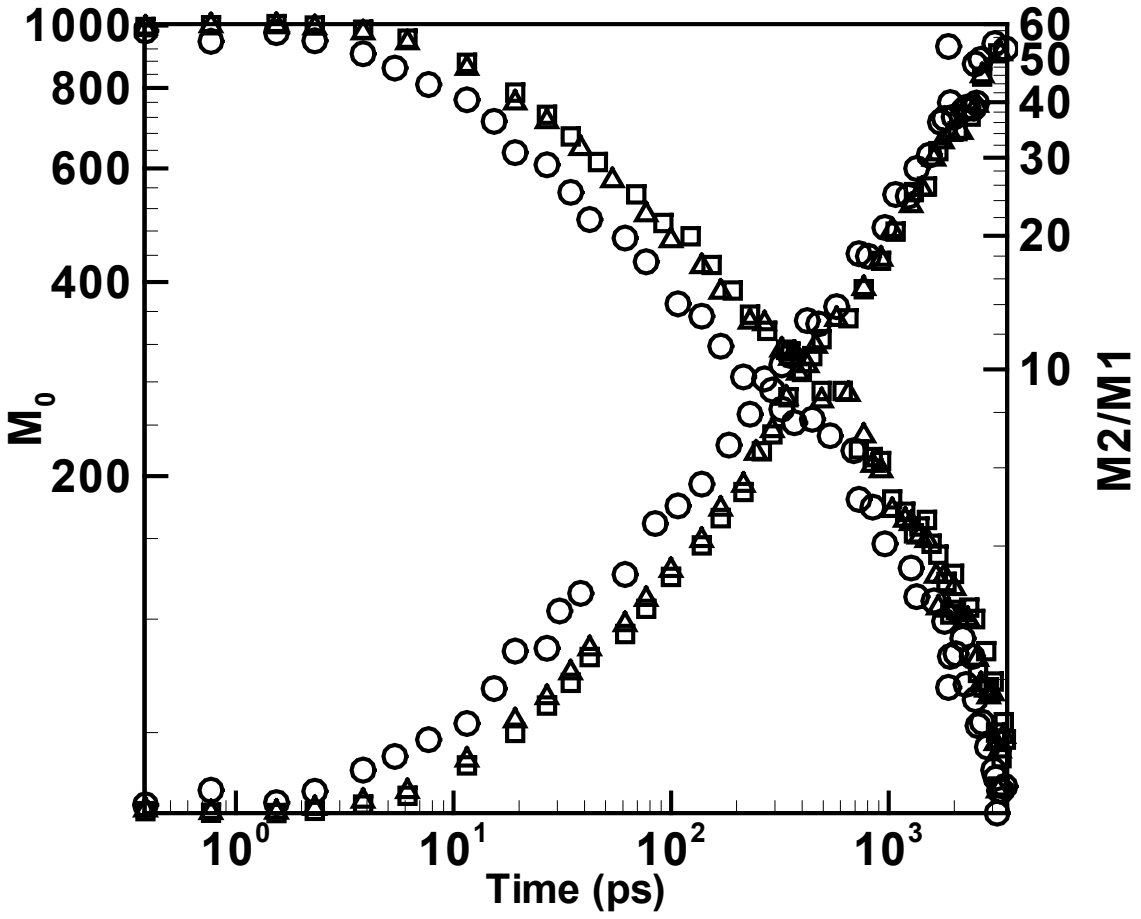

Figure XXX: Kapur, Prasad, and Sinno